Journal of Electroanalytical Chemistry 832 (2019) 399–407

Contents lists available at ScienceDirect

Journal of Electroanalytical Chemistry

journal homepage: www.elsevier.com/locate/jelechem

Electrochemistry of viologens at polypyrrole doped with sulfonated β–cyclodextrin

Valeria Annibaldi, Carmel B. Breslin*

Department of Chemistry, Maynooth University, Maynooth, Co. Kildare, Ireland

ARTICLE INFO

Keywords:
Polypyrrole
Viologens
Cyclodextrin
Paraquat
Cation exchange

ABSTRACT

The electrochemistry of methyl, ethyl and benzyl viologens was studied at polypyrrole doped with sulfonated cyclodextrin, PPysβ–CD, a cation exchange polymer. Three reduction waves were observed corresponding to the reduction of the viologen (V^{2+}) to the radical cation ($V^{\bullet+}$) followed by the neutral compound (V^0) and a third intense peak. This third reduction peak was associated with the ingress of V^{2+} as the PPysβ–CD film is reduced. As the incorporated V^{2+} is reduced to the neutral viologen, the influx of more V^{2+} occurs to achieve charge balance and this repeated influx and reduction of V^{2+} gives an intense reduction wave. These processes were only observed with sβ–CD as a dopant and this was attributed to the formation of an ion pair between the anionic cyclodextrin and the viologen. Lower diffusion coefficients and rate constants were observed for the reduction of V^{2+} and $V^{\bullet+}$ on adding an excess of sβ–CD to the viologen solution. Linear calibration curves were obtained extending from 1.0 μM to 80 μM when the PPysβ–CD was employed as a sensor for methyl viologen. While the PPysβ–CD is not suitable for the detection of low nM concentrations, the uptake and extraction of MV^{2+} was observed on polarising the PPysβ–CD in a solution of the viologen, highlighting the dual action of the polymer.

1. Introduction

Since their discovery in 1933 [1], there has been considerable interest in the applications of viologens, which are also known as 1,1′–disubstituted – 4,4′-bipyridine ions. They are widely used as electron transfer mediators in enzymatic reactions [2–4]. For example, Cosnier et al. [4] constructed a biosensor composed of polypyrrole functionalised with viologens with the ability to shuttle electrons between the electrode and the reactive centre of the enzyme, located deeply within the protein. Other applications include electrochromic materials, as the viologens can be easily switched between different colours [5,6]. Many of the viologens exhibit herbicidal activity, with methyl viologen being the most effective, and it is commonly known as paraquat [7]. Methyl viologen is a quick acting herbicide that destroys green plant tissue on contact, but it has also been recognised as an environmental toxin and its use is banned in a number of countries, including the European Union.

Viologens exist in three main oxidation states, as a dication, V^{2+}, a cationic radical, $V^{\bullet+}$, and the neutral state, V^0, with the dication being the most stable. The dication undergoes a one–electron reduction to generate the coloured radical cation, followed by a second one–electron reduction to form the neutral compound, which is frequently insoluble in aqueous solution. While the first reduction is known to be reversible, the second reduction is more complex, with several secondary reactions possible, including a conproportionation reaction between V^0 and V^{2+} to yield $V^{\bullet+}$, and dimerisation and disproportionation reactions of the $V^{\bullet+}$ [6]. The electrochemistry and electroreduction mechanisms of viologens have been studied extensively at gold and various carbon–-based electrodes [8,9].

Due to the toxic properties of methyl viologen and the fact that it is still employed in several countries, various analytical techniques have been used and developed for its detection. These range from HPLC and GC coupled with mass spectrometry to Raman spectroscopy, spectrofluourimetry and ELISA [10–14]. Electrochemical detection has also been employed and a number of modified electrodes has been used as sensors [15–19]. Recent examples include a phospholipid modified glassy carbon electrode [20], with a limit of detection of 2.2 nM. Carbon paste and modified carbon paste electrodes have also been employed giving detection limits in the region of 200 nM [21–23]. On the other hand, the removal and extraction of methyl viologen has attracted considerable interest [24–26]. Various materials with a high sorption capacity have been employed in an attempt to remove and extract methyl viologen from aqueous solutions [24–26].

In this study, polypyrrole doped with an anionic cyclodextrin was formed and used as a modified electrode for the reduction of methyl, ethyl and benzyl viologens. The cyclodextrin, with 7 to 11 sulfonate

* Corresponding author.
E-mail address: Carmel.Breslin@mu.ie (C.B. Breslin).

https://doi.org/10.1016/j.jelechem.2018.11.025
Received 11 August 2018; Received in revised form 15 November 2018; Accepted 15 November 2018
Available online 16 November 2018
1572-6657/

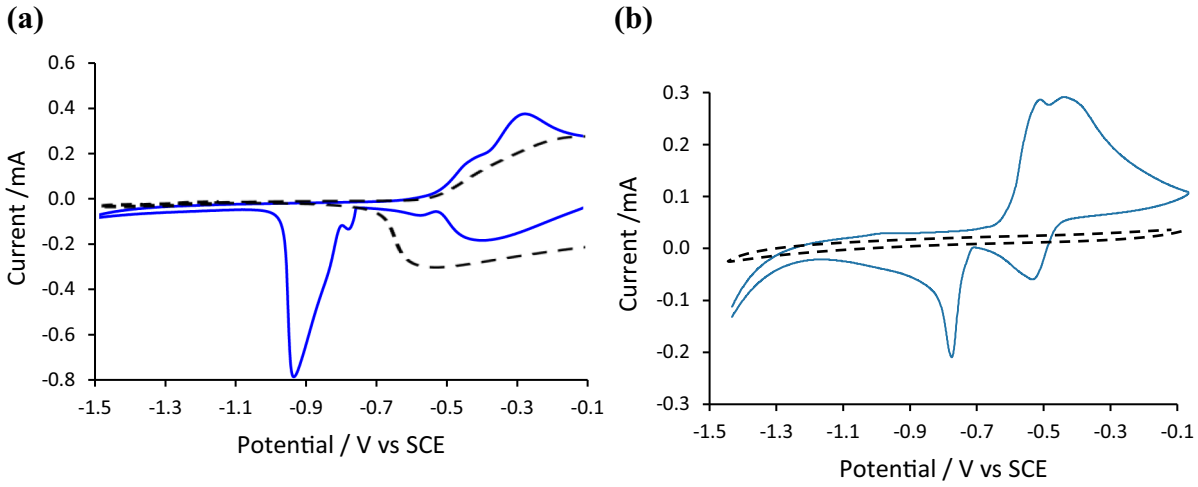

Fig. 1. (**a**) CV recorded for PPysβ–CD in 0.1 M NaCl at 50 mV s^{-1} in the absence (- - -) and presence (—) of 5.0 mM BV (**b**) CV recorded for Au in 0.1 M NaCl at 50 mV s^{-1} in the absence (- - -) and presence of (—) 5.0 mM BV.

groups per mole of cyclodextrin, is anionic and was employed to attract the cationic viologens. The dual action of this modified electrode as an electrochemical sensor and as a material capable of binding and extracting methyl viologen is briefly described.

2. Experimental

Cyclic voltammetry (CV) and constant potential amperometry were carried out using a Solartron 1287 potentiostat, while differential pulse voltammetry (DPV) and electrochemical quartz crystal microbalance measurements (EQCM) were performed using a CHi440 potentiostat. An EG&G, Model 636 ring disc electrode was used for the rotating disc voltammetry experiments. A standard three electrode cell was used consisting of a gold (3.0 mm) or glassy carbon (3.0 mm) working electrode, a high surface area platinum counter electrode and a saturated calomel reference electrode. The working electrodes were encased in an insulating Teflon sheath and electrical contact was maintained with a copper wire threaded into the base of the electrode. The electrodes were polished using a 1 μm Buehler monocrystalline diamond suspension on a Buehler microcloth, washed with deionised water and sonicated to remove any polishing residues. The EQCM electrochemical cell consisted of a custom–made Ag|AgCl reference, a gold quartz crystal electrode ($A = 0.203$ cm^2) obtained from IJ Cambria Scientific and a platinum wire counter electrode. The mass changes were calculated from changes in the measured frequency using the Sauerbrey equation, Eq. (1), where f_0 is the resonant frequency, Δm is the mass change, A is the surface area of the electrode, ρ_q is the density of quartz, 2.648 g cm^{-3}, and μ_q is the shear modulus of quartz, 2.947×10^{11} g cm^{-1} s^{-2}.

$$\Delta f = \frac{2f_0^2 \Delta m}{A(\rho_q \mu_q)^{1/2}} \quad (1)$$

When recording the DPV measurements, the pulse amplitude was set at 50.0 mV, pulse width at 0.10 s, sampling width at 0.05 s, pulse period at 0.30 s and increment at 3.0 mV. The uptake of methyl viologen was monitored using UV spectroscopy with a Cary 50 UV–Visible spectrometer.

All chemicals were obtained from Aldrich. Pyrrole was distilled under vacuum and stored at −20 °C in the dark to prevent oxidation, while the sulfonated β–cyclodextrin (sβ–CD) sodium salt was purified by dissolving the sample in a small amount of deionised water. The sample was then connected to a Schlenk line, dried under vacuum at a pressure of 0.01 mbar while stirring and heating at 70 °C for 12 h. All other chemicals were of analytical reagent grade and used without further purification. Deionised, Milli–Q, water was used for the preparation of all solutions and the solutions were deoxygenated with nitrogen for a 3–h period.

Pyrrole was electropolymerised in the presence of sβ–CD to generate the PPysβ–CD film [27]. A gold electrode was polarised at 0.60 V vs SCE in 0.2 M pyrrole dissolved in a 0.02 M sβ–CD solution, until a charge of 1.15C cm^{-2} was reached. For comparative purposes, polypyrrole was doped with dodecyl sulfate, PPySDS, by depositing the polymer from 0.2 M pyrrole in 0.02 M sodium dodecyl sulfate at 0.60 V vs SCE to a charge of 1.15C cm^{-2}. The PPysβ–CD modified electrodes were initially cycled from 0.0 V to −0.50 V vs SCE at 50 mV s^{-1} for 10 cycles in the viologen–containing solution, before the cyclic voltammograms or differential pulse voltammograms were recorded. This procedure was employed to incorporate V^{2+} within the polymer matrix using the cation exchange properties of the PPysβ–CD film. The viologens are inert within this potential window, while the polymer backbone is electroactive. All voltammograms presented, including CV, DPV and RDV, and EQCM data, are the average of 4 repeated experiments.

3. Results and discussion

As detailed earlier, the large sulfonated β–cyclodextrin, with 7 to 11 mol of sulfonate per mole of CD, is an immobile dopant, that is retained within the polymer matrix, giving the polymer cation exchange properties [28]. As the methyl (MV), ethyl (EV) and benzyl (BV) viologens are cationic, the electrochemistry of the viologens was studied at the PPysβ–CD modified electrode to determine if any interactions existed between the viologens and the polymer.

3.1. Electrochemistry of the viologens at PPysβ-CD

Cyclic voltammograms recorded at a PPysβ–CD modified gold electrode and an unmodified gold electrode in 5 mM BV are shown in Fig. 1. For comparative purposes the voltammograms recorded in the supporting electrolyte, 0.1 M NaCl, are shown. The electroactivity of PPysβ–CD is evident in the 0.1 M NaCl solution with a reduction wave, corresponding to the uptake of Na^+, at about −0.60 V vs SCE, while oxidation of the polymer is seen between −0.50 V and − 0.10 V vs SCE, Fig. 1(a). At potentials lower than −0.60 V vs SCE, there is no evidence of any redox reactions and the current remains low. There is a considerable change in the voltammogram on addition of BV to the chloride–containing solution. An intense reduction peak becomes apparent at about −0.92 V vs SCE and the electroactivity of the polymer

Table 1
Peak potentials (n = 4) for reduction of MV, EV and BV at a bare gold electrode and at PPysβ–CD.

Compound	Bare Au Potential/V vs SCE		PPysβ-CD Potential/V vs SCE		
	$V^{2+} + e^- \rightarrow V^{\bullet+}$ 1st reduction	$V^{\bullet+} + e^- \rightarrow V^0$ 2nd reduction	$V^{2+} + e^- \rightarrow V^{\bullet+}$ 1st reduction	$V^{\bullet+} + e^- \rightarrow V^0$ 2nd reduction	Adsorption peak
MV	−0.709	−1.042	−0.724	−1.033	−1.245
EV	−0.704	−1.040	−0.721	−0.988	−1.137
BV	−0.567	−0.790	−0.579	−0.770	−0.923

is altered between −0.60 V and − 0.10 V vs SCE. Furthermore, the voltammogram is very different to that recorded at gold, Fig. 1(b), where the first and second reduction peaks are clearly evident. The reduction of BV^{2+} to the radical species, $BV^{\bullet+}$ and the further reduction to BV^0 is also seen at the polymer, however the peaks are considerably smaller. It is difficult to obtain a reliable estimate of the charge associated with the reduction of BV^{2+} and $BV^{\bullet+}$ as some of the charge may be related to the redox activity of the polymer. However, it is clear that the charge consumed for the third reduction peak is considerably higher and this peak is not connected to the simple reduction of $BV^{\bullet+}$. Oxidation waves corresponding to the conversion of soluble BV^0 to $BV^{\bullet+}$, at about −0.10 V vs SCE, and its subsequent conversion to BV^{2+}, at approximately −0.32 V vs SCE, are evident, but are masked by the redox reactions of PPysβ–CD, which occur between −0.65 V and − 0.10 V vs SCE. It appears that the third reduction wave corresponds to an irreversible process. The peak potential values for the first and second reduction processes of the three viologen compounds are listed in Table 1 and compared to data collected at the bare gold electrode. In addition, the peak potential of the third reduction wave, which occurs only at the polymer–modified electrode, is reported.

The first reduction potential is slightly lower at the polymer–modified electrode, compared to the gold electrode. Shifts of 15 mV for MV, 17 mV for EV and 12 mV for BV, towards more negative potentials were recorded. These small shifts to more negative potentials may indicate an electrostatic interaction between the viologen compounds and the sulfonate groups on the sβ–CD dopants. Although the V^{2+} cations are incorporated and accumulated within the polymer matrix as the polymer is reduced to give relatively high concentrations that would normally facilitate reduction, the electrostatic interactions between the PPysβ–CD surface and the quaternary nitrogen of the viologens inhibit the reduction, shifting the reduction potentials to more negative values. In contrast, the second reduction of BV and EV is slightly more facile at the polymer surface. An electropositive shift of 52 mV is evident with EV, while $BV^{\bullet+}$ is reduced at −0.77 V vs SCE, to give a positive potential shift of 20 mV with respect to the bare electrode. This can be explained in terms of the accumulation of the radical species in the polymer matrix. As the PPysβ–CD has a porous structure, the generated radicals may be trapped and accumulate within the polymer matrix. This accumulation and local increase in the concentration of the radical species would account for the easier reduction.

This intense reduction peak was also evident using DPV. Typical voltammograms are shown in Fig. 2(a) for PPysβ–CD cycled in 0.05 M NaCl in the presence and absence of 1 mM EV. Again, three reduction peaks are evident. The first peak, around −0.70 V vs SCE, corresponds to the reduction of the dication to generate the radical species ($EV^{2+} + e^- \rightarrow EV^{\bullet+}$), the signal, which appears as a shoulder peak, at −1.05 V vs SCE was assigned to the second reduction ($EV^{\bullet+} + e^- \rightarrow EV^0$). The large wave at −1.20 V vs SCE is observed again. It is also evident that the current due to the polymer electroactivity is substantially diminished in the presence of the viologens. This may indicate competition between the cationic viologen and the sodium cations from the supporting electrolyte for uptake into the polymer.

The electrochemistry of the viologens at PPysβ–CD was compared to polypyrrole doped with a large non–macrocyclic anion, sodium dodecyl sulfate (SDS). The SDS anions are large bulky dopants, which give the polypyrrole cation exchange properties. The SDS–doped polymer (PPySDS) showed no evidence of the electrochemistry of the viologens, Fig. 2 (b), where the trace recorded in the NaCl solution is nearly identical to that obtained in the viologen–containing solution. The significant variation between PPySDS and PPysβ–CD may be due to the different amount of negative charge possessed by the two dopants. The sβ–CD has an average of 9 sulfonate groups per molecule and it is likely that some of these anionic groups remain free and not involved in charge compensation, as this would place too much strain on the dopant and the polymer matrix. Indeed, Naoi and co–workers [29], in studying the doping of polypyrrole with mono–, di– and tri–sulfonated

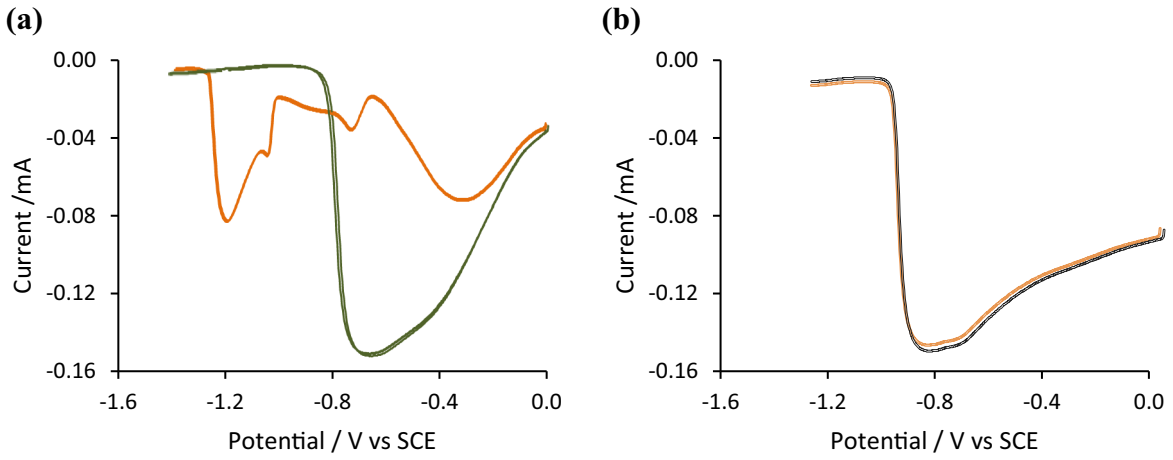

Fig. 2. (**a**) DPV of PPysβ–CD in 0.05 M NaCl in the absence (—) and presence (—) of 1.0 mM EV (b) DPV of PPySDS in 0.05 M NaCl in the absence (—) and presence (—) of 1.0 mM EV.

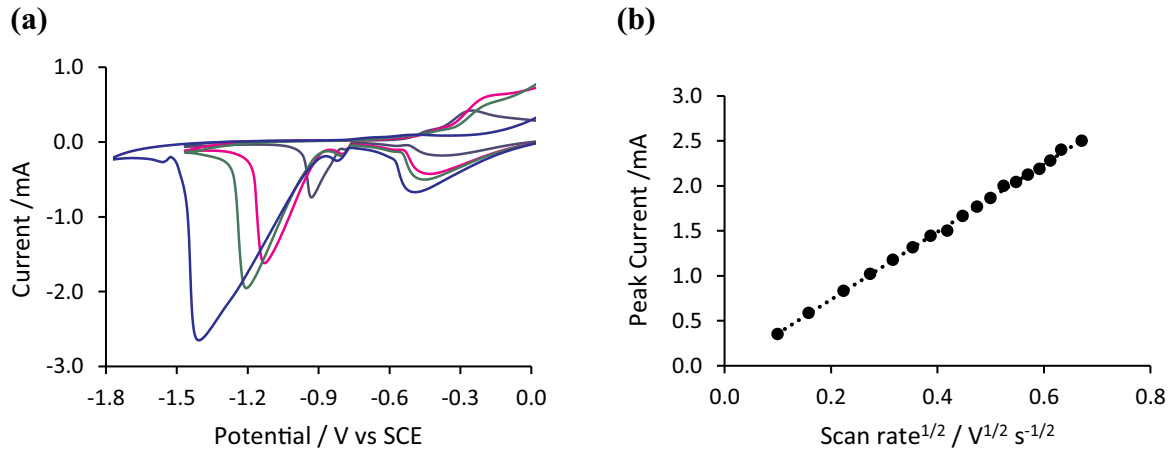

Fig. 3. (a) Cyclic voltammograms recorded for 5.0 mM BV in 0.10 M NaCl at scan rates of 50, 150, 200 and 400 mV s^{-1} at PPysβ–CD **(b)** peak current for the third reduction wave plotted as a function of the square root of the scan rate.

naphthalene, concluded that the PPy–trisulfonate doped films possessed free sulfonated groups without any charge compensation.

It is clear that the intense reduction peaks observed in the voltammograms are due to the presence of the sβ–CD dopant. Indeed, the peak current depended on the thickness of the PPysβ–CD films, with the peak current increasing for polymers deposited to higher charges. These thicker polymer films have a higher concentration of sβ–CD dopants, a higher surface area and possibly a more porous surface, facilitating a greater interaction with the charged viologens. This intense peak has the typical shape and asymmetry of a redox process involving adsorbed species. On increasing the scan rate a substantial shift in the peak potential was observed as illustrated in Fig. 3(a), while the first and second reduction waves are minimally affected by the increasing scan rate. This large shift of the peak potential indicates a slow and irreversible process. However, a linear relationship between the peak current and the square root of the scan rate was obtained, Fig. 3(b), indicating a diffusion–controlled process. This indicates that the third intense wave represents a complex process that exhibits characteristics of adsorption and diffusion.

In an attempt to obtain more information on this adsorption process, quartz crystal microbalance experiments for PPysβ–CD cycled in different concentrations of BV were carried out and the results are summarised in Fig. 4. For the data presented in Fig. 4(a), the potential was cycled from 0.0 V to −1.20 V vs Ag|AgCl. When the polymer was cycled in 5.0 mM BV with a 0.1 M NaCl supporting electrolyte, three linear regions exhibiting different slopes could be identified, as shown in Fig. 4(a). The first fragment is connected with the electroactivity of polypyrrole, where the ingress of BV^{2+} and Na^{+} occurs. At approximately −0.60 V vs Ag|AgCl the slope of the mass plot changes. This second section of mass increase occurs from −0.60 V to −0.80 V vs Ag|AgCl which is the potential region corresponding to the first and second reduction of the BV at the polymer–modified electrode. Finally, the potential window for the last portion is observed from −0.80 V to −1.20 V vs Ag|AgCl and this is related to the third intense reduction peak. In the absence of BV, the mass remains essentially constant between −0.60 V and − 0.80 V vs Ag/AgCl with a slight reduction in the overall mass, indicating no further uptake of Na^{+} or water molecules, and possibly the loss of some water molecules. The final mass change recorded at −1.2 V vs Ag|AgCl was approximately 1.0 μg. The mass change observed in the presence of 5.0 mM BV was 7.23 μg and on reduction of the BV concentration to 2.5 mM, the mass change involved in the overall process was nearly halved, 3.05 μg, showing a clear relationship between the mass deposited and the concentration of BV in solution. Clearly, there is a considerable increase in mass as the polymer is cycled in the BV–containing solutions. Both the radical and the neutral species generated from the reduction of the viologen within the solution are deposited to some extent on the polymer, however a more substantial mass increase is observed from −0.80 V to −1.20 V

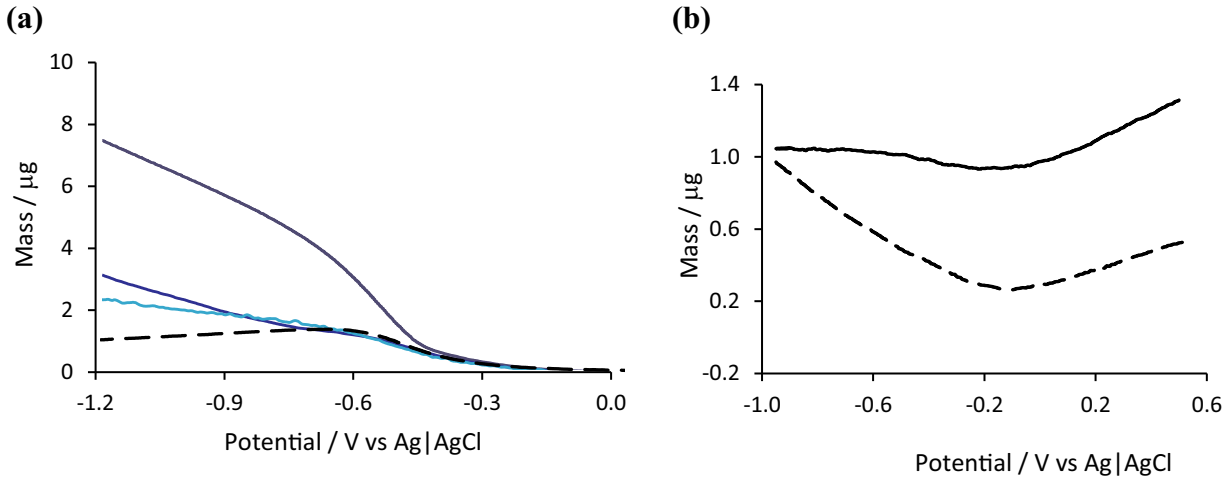

Fig. 4. EQCM data recorded at 50 mV s^{-1} for PPysβ–CD in **(a)** 0.1 M NaCl and (– –) 0 mM BV, (—) 1.0 mM BV, (—) 2.5 mM BV and (—) 5.0 mM BV, **(b)** reverse scan in 0.1 M NaCl and (– –) 0 mM BV and (—) 5.0 mM BV.

vs Ag|AgCl. This mass increase and the corresponding large reduction wave, seen in Figs. 1 and 2, seem to be connected to the ingress of BV^{2+} and deposition of BV^{0} at the polymer. As the PPysβ–CD is reduced, BV^{2+} is incorporated to balance the charge and maintain electroneutrality, as illustrated in Eq. (2).

$$PPy^{n+}\left(\frac{n}{m}\right)s\beta\text{–}CD^{m-} + \left(\frac{n-b}{2}\right)BV^{2+} + (b)Na^{+} + ze^{-} \rightarrow$$
$$PPy^{0}\left(\frac{n}{m}\right)s\beta\text{–}CD^{m-}\left(\frac{n-b}{2}\right)BV^{2+}(b)Na^{+} \quad (2)$$

As the BV^{2+} is electroactive it is reduced to $BV^{\bullet+}$ and then BV^{0} and as this reaction proceeds it gives rise to the accumulation of BV^{0} at the PPysβ–CD surface. As the anionic cyclodextrin is immobile more cations are required for charge balance and further ingress of BV^{2+} and Na^{+} occurs and again the incorporated BV^{2+} is reduced, leading to the repeated ingress and reduction of BV^{2+}. In addition, conproportionation reactions are well known to occur with viologens [10] and as the concentration of BV^{0} increases it may undergo a conproportionation reaction with the dication BV^{2+}, which is the predominant species within the bulk solution. This conproportionation reaction generates more radicals which, in turn, are reduced in a cyclic reaction. As the result of the repeated ingress and reduction of the viologen and the potential conproportionation reactions, an intense peak is observed which has the characteristics of an adsorption process. The EQCM data shown in Fig. 4(b) were recorded during the reverse oxidation cycle and the potential was cycled to 0.60 V vs SCE. The initial mass in the BV solution was recorded as 6.4 μg at −1.0 V vs Ag|AgCl, but this was set to 1.0 μg for ease of presentation. In the absence of BV, a clear mass decrease was observed between −1.0 V and −0.20 V vs Ag|AgCl which is consistent with the egress of Na^{+} and its associated solvated water molecules, while the small mass increase at the higher potentials is associated with ingress of chloride anions. The data recorded in the presence of BV, show little or no evidence for the removal of BV from the polymer. The small mass loss observed between −1.0 V and −0.20 V vs Ag|AgCl is probably connected with the expulsion of BV^{2+} or Na^{+} and at the higher potentials chloride anions are incorporated as the polymer is further oxidised. This shows that the incorporation of chloride anions occurs even though a relatively high concentration of BV is trapped within the polymer matrix. These data are in good agreement with the voltammograms presented in Figs. 1 and 2, which clearly show that this third reduction is irreversible and the reduced BV is not released from the polymer matrix. It is well known that the reduced and neutral BV^{0} has poor solubility in water [6] and as higher amounts of BV^{2+} are incorporated and reduced to BV^{0} an irreversible reduction wave becomes apparent.

It is evident from the voltammograms, Figs. 1 to 4, that the third reduction wave associated with the viologens occurs at potentials where the polymer is reduced. Normally under these conditions the polymer becomes insulating. However, the reduced PPysβ–CD contains a network of cations, Eq. (2), and this, combined with the porous nature of the polymer, will facilitate the reduction of the viologen at the gold substrate and possibly throughout the polymer matrix. As the sβ–CD dopant is large and bulky it is likely to give a more porous polymer matrix, compared to simple dopants, such as chlorides. It appears that the cation exchange properties of the polymer, combined with a high number of anionic pendants on the rim of the CD cavity and the porous nature of the polymer matrix, provide a surface that is capable of binding and reducing the viologens.

3.2. Electrostatic interactions between viologens and sβ–CD

In addition to the intense reduction wave, it was found that the background signal for the polymer electroactivity increased as the viologen concentration was decreased. This was observed with both CV and DPV measurements and is illustrated in Fig. 5 for the

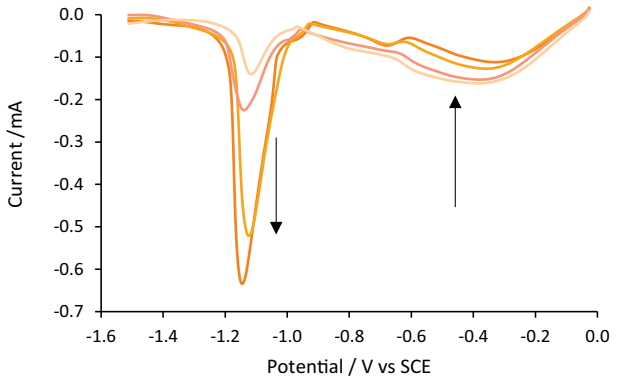

Fig. 5. Cyclic voltammograms recorded at 50 mV s^{-1} for PPsβ–CD in 5.0 mM, 4.0 mM, 1.5 mM and 1.0 mM EV in 0.1 M NaCl.

EV–containing solutions. The arrows shown on the plot indicate the direction of the current change on increasing the concentration of EV. It is clearly visible from the plot that the current for the polymer electroactivity, between −0.10 V and −0.60 V vs SCE, decreases as the EV concentration increases. In this potential interval the viologens are present in solution as dications. When reduction of the polymer takes place an influx of cations, with competition between Na^{+} and the EV^{2+}, occurs in order to maintain the electroneutrality of the polypyrrole backbone. Higher concentrations of the viologen promote the dication exchange over the Na^{+} exchange. The data shown in Fig. 5 represent the first cycle and the polymer is cycled from 0.0 V to −1.5 V vs SCE. Therefore, the lower currents observed for the redox properties of the polymer are not due to the deposition of insoluble EV^{0}. Instead, they are probably related to the lower mobility of the viologen compared to the Na^{+} cation, where the lower mobility gives rise to a slower reduction of the polymer.

The electrostatic interaction between sβ–CD and MV was studied in solution using rotating disc voltammetry. The electrochemistry of the viologen in the presence of varying concentrations of sβ–CD was monitored at different rotation rates. The diffusion coefficients and heterogeneous rate constants for free MV in the absence and presence of excess sβ–CD were calculated using the Levich, Eq. (3), and Koutecky–Levich, Eq. (4), equations. In this analysis, F is Faraday's constant, A is the surface area, k is the rate constant, Γ is the surface coverage, c is the concentration, D is the diffusion coefficient, ω is the rotational speed and ν is the kinematic viscosity. In Eq. (4), i_L represents the measured limiting current and i_{lev} is the Levich current.

$$i_L = 0.621nFAD^{2/3}\nu^{-1/6}c\omega^{-1/2} \quad (3)$$

$$\frac{1}{i_L} = \frac{1}{i_K} + \frac{i}{i_{lev}} = \frac{1}{nFAkc} + \frac{1.61}{nFA\nu^{-1/6}D^{2/3}\omega^{1/2}c} \quad (4)$$

In addition, the binding constant, K_f, between MV and the sβ–CD was estimated by fitting the half–wave potential shifts, $\Delta E_{1/2}$, and the D_c/D_f ratios to Eq. (5), where $(E_{1/2})_f$ and $(E_{1/2})_c$ are the half–wave potentials for the free and for the complexed analyte, respectively, D_f is the diffusion coefficient of the free viologen while D_c is the diffusion coefficient of the viologen in the presence of sβ–CD.

$$\left(\frac{F}{RT}\right)\{(E_{1/2})_c - (E_{1/2})_f\} = \ln(1 + K_f[CD]) + \ln\left(\frac{D_c}{D_f}\right)^{1/2} \quad (5)$$

Rotating disc voltammograms are shown in Fig. 6 for MV in the presence and absence of the sβ–CD, while a cyclic voltammogram recorded at the GC electrode in a 40 mM sβ–CD containing chloride solution is shown in the inset. This voltammogram clearly shows that the cyclodextrin is stable at these low applied potentials. It is evident from the rotating disc voltammograms, that the addition of the cyclodextrin has a significant effect on the reduction of MV. The limiting currents are

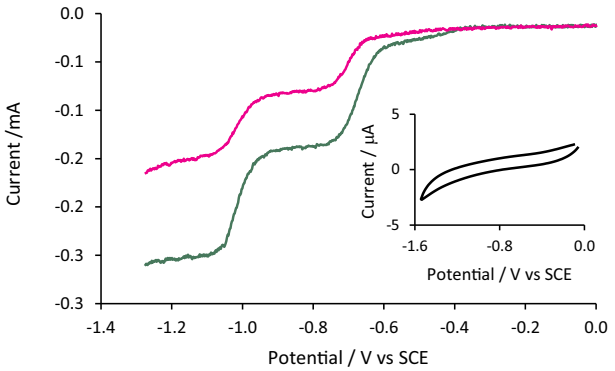

Fig. 6. RDV voltammograms of 1.0 mM MV in 0.1 M NaCl on a GC disc electrode at 50 mV s^{-1} and 2000 rpm in the absence (—) and presence (—) of 40 mM sβ–CD. Inset shows a voltammogram recorded at GC in 0.1 M NaCl and 40 mM sβ–CD at 50 mV s^{-1}.

lower and there is a shift in the half–wave reduction potential. With a 40–fold excess of sβ–CD a negative shift in the half–wave potential, $\Delta E_{1/2}$, of 45 mV vs SCE, was observed for the reduction of the dication to form the radical, $MV^{2+} + e^- \rightarrow MV^{\bullet+}$. A similar shift of 38 mV vs SCE was observed for the reduction of the radical to the neutral molecule, $MV^{\bullet+} + e^- \rightarrow MV^0$.

In Fig. 7, Levich plots for MV free and for the analyte in solution with a 40–fold excess of sβ–CD are presented and again it is evident that the sβ–CD has an influence on the diffusion coefficient. For the free MV, diffusion coefficients, D_f, of 4.91×10^{-6} cm^2 s^{-1} and 5.78×10^{-6} cm^2 s^{-1} were computed for the dication and radical species, respectively. These values are in good agreement with work published by Ling et al. [30]. Lower diffusion coefficients were calculated for the viologens with sβ–CD. A diffusion coefficient equal to 2.10×10^{-6} cm^2 s^{-1} was obtained for the MV^{2+}, while a value of 2.74×10^{-6} cm^2 s^{-1} was calculated for the $MV^{\bullet+}$ species in the presence of an excess of sβ–CD, giving D_c/D_f ratios of 0.43 and 0.47 for the MV^{2+} and $MV^{\bullet+}$, respectively. Ratios, D_c/D_f, of 0.47 have been reported in the literature and are usually taken to confirm an inclusion complex or some other form of an association complex with a large bulky molecule, such as a cyclodextrin [31,32]. Koutecky–Levich plots for MV free and in the presence of sβ–CD are shown in Fig. 8. Again, it is clear that the rate constant is influenced by the added sβ–CD. The rate constant was calculated as 0.113 cm s^{-1} for free MV^{2+}, in perfect agreement with that published by Ling et al. [30]. A lower rate constant of 0.024 cm s^{-1} was observed for the MV^{2+} in the presence of sβ–CD. Likewise, the rate constant for the second reduction reaction, $MV^{\bullet+} + e^- \rightarrow MV^0$, was reduced from 0.045 cm s^{-1} to 0.011 cm s^{-1} in the presence of sβ–CD.

Using the shifts in the half–wave potentials and Eq. (5), K_f values of 195 ± 5 M^{-1} for MV^{2+} and 115 ± 4 M^{-1} for $MV^{\bullet+}$ were calculated. These values combined with the changes in the diffusion coefficients and rate constants clearly confirm interactions between the charged viologens and the anionic cyclodextrin, with a somewhat stronger interaction between MV^{2+} and the cyclodextrin. This is consistent with the more negative reduction potentials observed for the reduction of MV^{2+}, Table 1, while the accumulation of $MV^{\bullet+}$ within the polymer matrix exceeds the weaker electrostatic interactions with the sβ–CD, giving rise to more positive reduction potentials for the second reduction wave, Table 1. This interaction appears to be electrostatic with the formation of an ion pair as opposed to a host–guest inclusion complex. It is often reported that K_f values of several hundred are associated with a moderate affinity of the guest for the host, while a strong inclusion complex is confirmed with K_f values larger than about 1000 M^{-1} [33].

3.3. Detection of viologens and calibration curves

The potential of PPysβ–CD to act as a sensor for the viologens was studied briefly using CV, DPV and constant potential amperometry, CPA. Calibration curves were generated using a 0.05 M NaCl supporting electrolyte to minimise competition with the viologens. Using cyclic voltammetry and following the intense reduction peak, linear calibration curves were obtained, however the reduction peak decreased rapidly with concentration and peak currents for concentrations lower than 0.05 mM were difficult to measure. This may be related to competition between the uptake of Na^+ and the V^{2+} and as the viologen concentration is reduced, higher concentrations of Na^+ are incorporated. Instead, the electroactivity of the polymer was used to follow the viologen concentrations. As evident in Figs. 2 and 5 the electroactivity of the polymer is seen between −0.10 V and approximately −0.70 V vs SCE and varies with the concentration of the viologen. A typical calibration curve is shown in Fig. 9(a), where the MV concentration is plotted as a function of the background current of PPysβ–CD, where the current was recorded at −0.60 V vs SCE. Good linearity was obtained for all three viologen compounds. For ethyl viologen, good linearity was observed down to 100 µM and more satisfactory results were obtained for methyl and benzyl viologens with linear relationships down to 20 µM and 25 µM, respectively. The CPA experiments were carried out at a constant potential of −0.90 V vs SCE, corresponding to the reduction of MV^{2+} to the radical cation ($MV^{2+} + e^- \rightarrow MV^{\bullet+}$). The current was measured before and after the addition of measured aliquots of methyl viologen to a 0.05 M NaCl electrolyte solution. The linear calibration curve is depicted in Fig. 9(b),

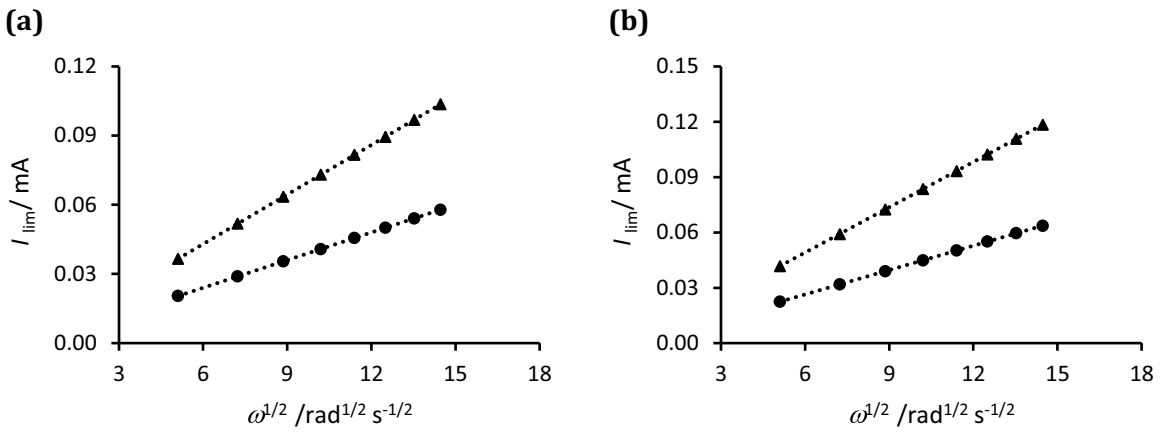

Fig. 7. Levich plots for the limiting currents of the first (**a**) and second (**b**) reduction waves of 1.0 mM MV in 0.1 M NaCl on a GC electrode at 50 mV s^{-1} in the absence (▲) and presence (●) of 40 mM sβ–CD.

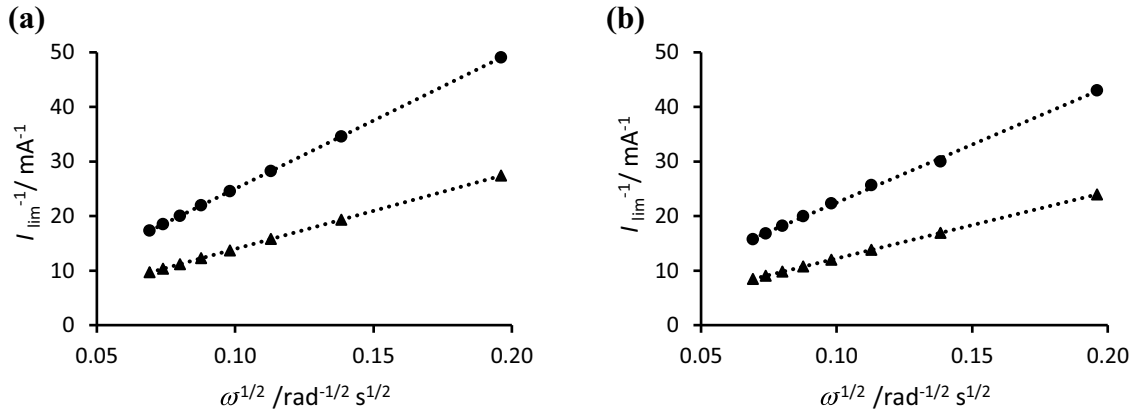

Fig. 8. Koutechy–Levich plots for the limiting currents of the first (**a**) and second (**b**) reduction waves of 1.0 mM MV in 0.1 M NaCl on a GC electrode at 50 mV s^{-1} in the absence (▲) and presence (●) of 40 mM sβ–CD.

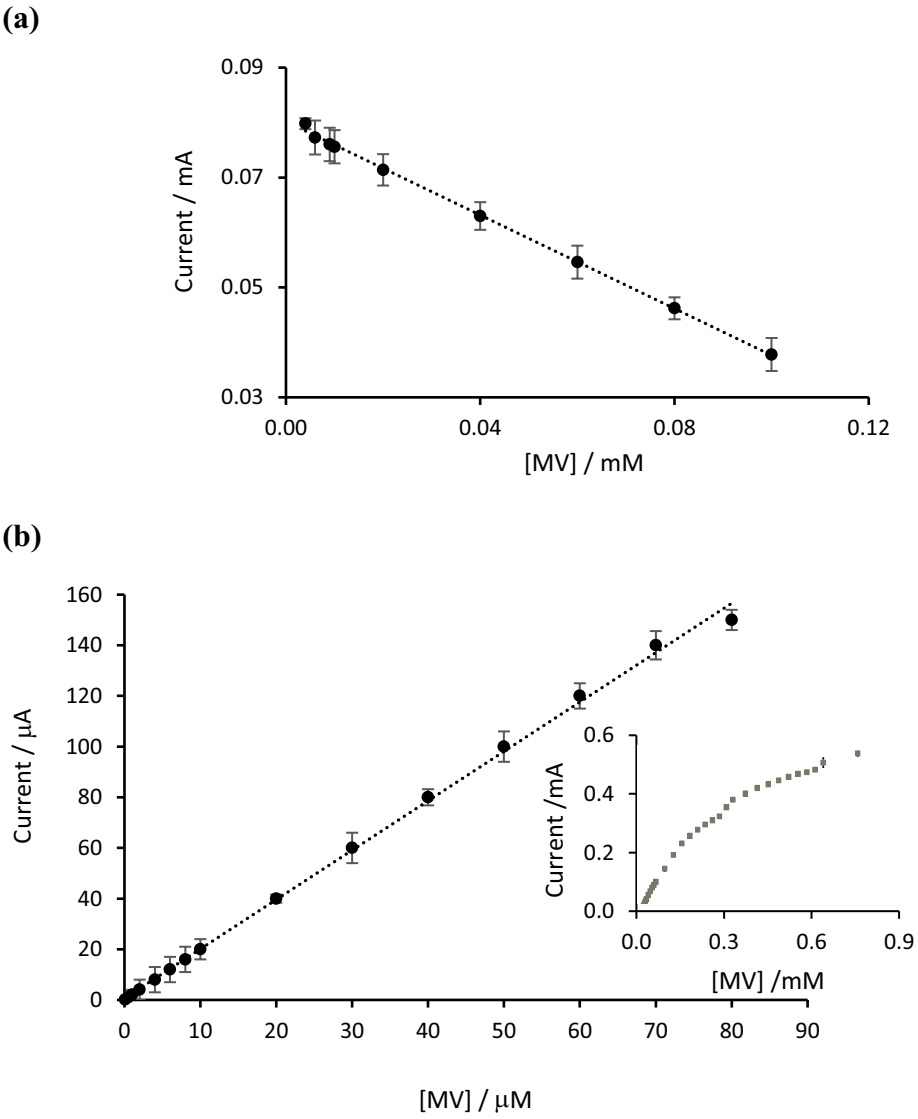

Fig. 9. (**a**) Background currents recorded using DPV of PPysβ–CD as a function of the MV concentrations ($n = 4$) (**b**) Limiting currents using CPA at −0.90 V vs SCE as a function of the MV concentration for the reduction of MV^{2+} to $MV^{\bullet+}$ at the PPysβ–CD modified electrode ($n = 4$).

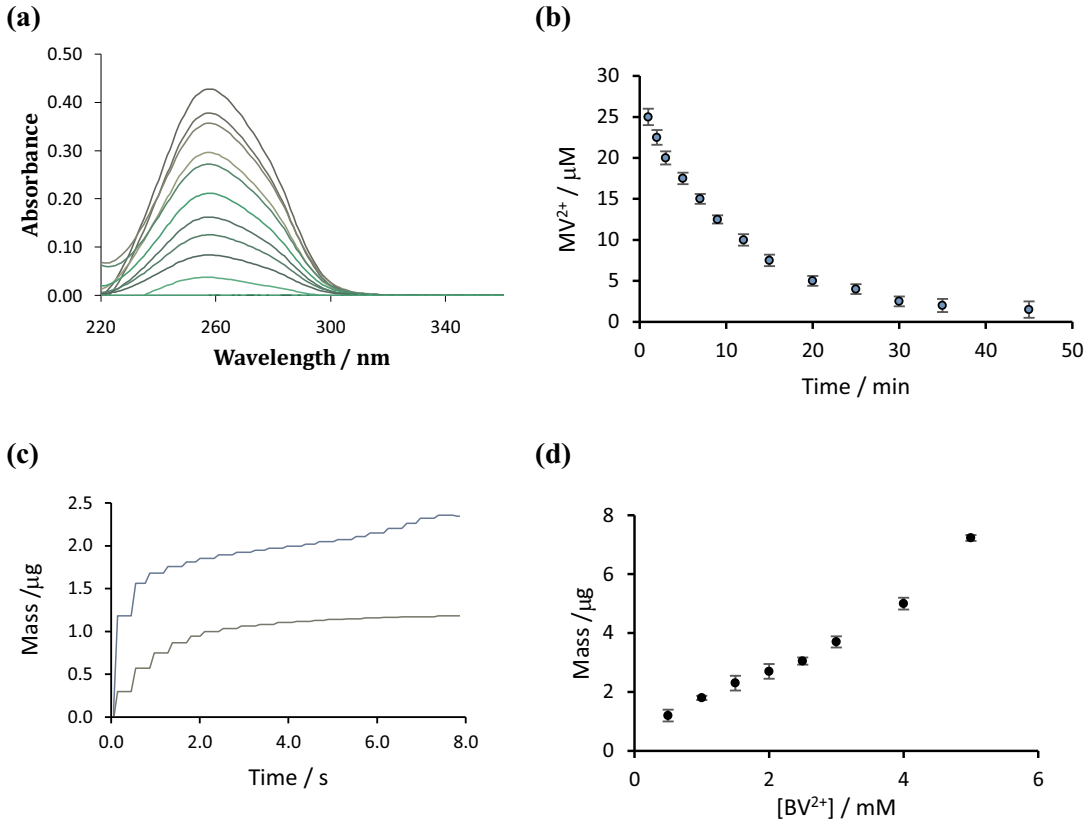

Fig. 10. (**a**) UV absorbance plots of MV^{2+} recorded as a function of time (from 0 to 45 min) exposed to PPysβ–CD polarised at −0.65 V vs SCE, (**b**) concentration of MV^{2+} plotted as a function of the polarisation period (n = 4), (**c**) EQCM data recorded on polarisation of PPysβ–CD at −1.0 V vs SCE in 1.0 M NaCl in the absence (—) and presence (—) of 1.5 mM BV and (**d**) mass uptake as a function of BV^{2+} concentration in 0.1 M NaCl, (n = 4).

where the steady–state current is plotted as a function of the MV^{2+} concentration, while the plot obtained at higher concentrations is shown in the inset and shows that the data deviate from linearity at the higher concentrations. The linear plot was maintained to a concentration of 1.0 µM. Using Eq. (6), where m is the sensitivity and S_b is the standard deviation of the background current, the calculated limit of detection was computed as 0.85 µM. While linear calibration curves were obtained over a wide concentration range, with reasonable detection limits of about 850 nM, these detection limits are not sufficient for the analysis of low nM MV^{2+} levels.

$$C_m = \frac{3S_b}{m} \tag{6}$$

3.4. Uptake and removal of viologens

The electrostatic interactions between the viologens and the PPysβ–CD were studied for the uptake and removal of MV^{2+} and BV^{2+}. EQCM was used to study the uptake of BV^{2+} by monitoring mass changes with thin polymer films, while UV–visible spectroscopy was employed to monitor the removal of MV^{2+} using the bulk PPysβ–CD films. These data are summarised in Fig. 10. In Fig. 10(a) UV data are shown for MV^{2+} exposed to PPysβ–CD polarised at −0.65 V vs SCE. The data show the decay in the concentration with increasing exposure times and clearly show the removal of MV^{2+}. At this potential the PPysβ–CD film is reduced and the MV^{2+} is incorporated to maintain charge neutrality. The electrostatic interactions with the anionic sβ–CD maintain both the MV^{2+} and any $MV^{\bullet+}$, that is generated on reduction, within the polymer matrix. In Fig. 10(b), the concentration of MV^{2+} is plotted as a function of the uptake period and shows that most of the MV^{2+} is removed and retained within the polymer matrix within a 40 min period. Using these experimental conditions (10 mL volume), a total of 2.4×10^{-7} mol of MV^{2+} were bound to the bulk polymer.

The data presented in Fig. 10(c) show the mass–time plots for PPysβ–CD polarised at −1.0 V vs Ag|AgCl in a high concentration of 1.0 M NaCl and in 1.5 mM BV in the presence of 0.1 M NaCl. At this potential, the polymer is reduced and requires the uptake of cations and this is evident in the chloride solution where the mass increase after 8 s is about 1 µg. In the presence of BV, a more significant mass increase is evident during the first 2 s and this indicates the incorporation of BV^{2+} with a larger mass. Then the mass remains essentially constant until a further increase is seen at about 6 s. Again, this mass increase may be associated with the reduction of BV^{2+} trapped within the polymer matrix to give BV^0, which in turn is deposited within the polymer, or at the gold substrate. As the positively charged BV^{2+} is removed, a further ingress of cations, Na^+ and BV^{2+}, is required to balance the charge on the sβ–CD. These processes enable the incorporation and deposition of the neutral viologen. The mass changes recorded on polarisation of PPysβ–CD at −1.0 V vs SCE in solutions of varying BV^{2+} concentrations are shown in Fig. 10(d). It is clear that increasing amounts of BV^0 are deposited with increasing concentration. These data clearly show that the PPysβ–CD film has potential applications in the removal and uptake of viologens. The uptake of the viologen as V^{2+} is achieved on reduction of the polymer, while the neutral V^0 is deposited on the application of lower applied potentials.

4. Conclusions

Polypyrrole was doped with sβ–CD, a large anionic cyclodextrin, to give a cation exchange conducting polymer, PPysβ–CD. On cycling the polymer in MV, EV and BV–containing solutions, the reduction of V^{2+} to $V^{\bullet+}$ and the subsequent reduction of $V^{\bullet+}$ to V^0 were observed for all

three viologens. In addition, a third large reduction wave was observed that indicated a slow irreversible process. This large reduction wave was linked to the reduction of the polymer and the accumulation of the reduced viologen. On reduction of the PPysβ–CD film, V^{2+} cations are incorporated and then reduced to V^0 as the potential is made more negative. As the cationic species are reduced to neutral molecules, more viologen cations are incorporated to maintain charge balance and reduced to give a cyclic effect of V^{2+} ingress and reduction. Furthermore, as V^0 is accumulated, a conproportionation reaction between V^0 and V^{2+} may occur to give more radical cations which, in turn, are reduced. This irreversible third reduction wave appears to be associated with the deposition of the poorly water soluble neutral viologen, V^0. The redox properties of the PPysβ–CD film will be altered as higher amounts of the insoluble V^0 are deposited within the polymer matrix. However, these water insoluble viologens can be dissolved by placing the polymer in a suitable organic solvent.

Using rotating disc voltammetry, the electrochemistry of MV^{2+} in the presence of excess sβ–CD showed evidence for the formation of an ion pair. These interactions were employed in the extraction of MV^{2+} from solution. On reduction of the polymer the MV^{2+} was incorporated within the polymer matrix and removed from solution.

Acknowledgements

The authors would like to acknowledge Science Foundation Ireland (SFI) for funding this work.

References

[1] L. Michaelis, E.S. Hill, The viologen indicators, J. Gen. Physiol. 16 (1933) 859–873.
[2] P.D. Hale, L.I. Boguslavsky, H.I. Karan, H.L. Han, H.S. Lee, Y. Okamoto, T.A. Skotheim, Investigation of viologen derivatives as electron-transfer mediators in amperometric glucose sensors, Anal. Chim. Acta 248 (1991) 155–161.
[3] C. Gomez–Morena, M.T. Bes, Structural requirements for the electron transfer between a flavoprotein and viologens, Biochim. Biophys. Acta Bioenerg. 1187 (1994) 236–240.
[4] S. Cosnier, B. Galland, C. Innocent, New electropolymerizable amphiphilic viologens for the immobilization and electrical wiring of a nitrate reductase, J. Electroanal. Chem. 433 (1997) 113–119.
[5] M. Vidotti, S.I. Cordoba de Torresi, Nanochromics: old materials, new structures and architectures for high performance devices, J. Braz. Chem. Soc. 19 (2008) 1248–1257.
[6] R.J. Mortimer, Electrochromic materials, Chem. Soc. Rev. 26 (1997) 147–156.
[7] M.A. Bacigalupo, G. Meroni, M. Mirasoli, D. Parisi, R. Longhi, Ultrasensitive quantitative determination of paraquat: application to river, ground and drinking water analysis in an agricultural area, J. Agric. Food Chem. 53 (2005) 216–219.
[8] E.E. Engelman, D.H. Evans, Investigation of the nature of electrodeposited neutral viologens formed by reduction of the dications, J. Electroanal. Chem. 349 (1993) 141–158.
[9] C.L. Bird, A.T. Kuhn, Electrochemistry of the viologens, Chem. Soc. Rev. 10 (1981) 49–82.
[10] N. Masque, M. Galia, R.M. Marce, F. Borrull, Chemically modified polymeric resin used as sorbent in a solid–phase extraction process to determine phenolic compounds in water, J. Chromatogr. A 771 (1997) 55–61.
[11] T.L. Kuo, D.L. Lin, R.H. Liu, F. Moriya, Y. Hashimoto, Spectra interference between diquat and paraquat by second derivative spectrophotometry, Forensic Sci. Int. 121 (2001) 134–139.
[12] P. Shivhare, V.K. Gupta, Spectrophotometric method for the determination of paraquat in water, grain and plant materials, Analyst 116 (1991) 391–393.
[13] M. Ibanez, Y. Pico, J. Manes, Online liquid chromatographic trace enrichment and high–performance liquid chromatographic determination of diquat, paraquat and difenzoquat in water, J. Chromatogr. A 728 (1996) 325–331.
[14] R.D. Whitehead Jr., M.A. Montesano, N.K. Jayatilaka, B. Buckley, B. Winnik, L.L. Needham, D.B. Barr, Method for measurements of the quaternary amine compounds paraquat and diquat in human urine high–performance liquid chromatography–tandem mass spectrometry, J. Chromatogr. B 878 (2010) 2548–2553.
[15] T.H. Lu, I.W. Sun, Electrocatalytic determination of paraquat using a nafion film coated glassy carbon electrode, Talanta 53 (2000) 443–451.
[16] J.M. Zen, S.H. Jeng, H.J. Chen, Determination of paraquat by square–wave voltammetry at a perfluorosulfonated ionomer/clay–modified electrode, Anal. Chem. 68 (1996) 498–502.
[17] M.A. El Mhammedi, M. Bakasse, A. Chitaint, Electrochemical studies and square wave voltammetry of paraquat at natural phosphate modified carbon paste electrode, J. Hazard. Mater. 145 (2007) 1–7.
[18] M. Luque, A. Rios, M. Valcarcel, Sensitive determination of paraquat and diquat at the sub–ng mL^{-1} level by continuous amperometric flow methods, Analyst 123 (1998) 2383–2387.
[19] T. Nasir, G. Herzog, M. Hebrant, C. Despas, L. Liu, A. Walcarius, Mesoporous silica thin films for improved electrochemical detection of paraquat, ACS Sens. 3 (2018) 484–493.
[20] H. Tomkova, R. Sokolova, T. Opletal, P. Kucerova, L. Kucera, J. Souckova, J. Skopalova, P. Bartak, Electrohemical sensor based on phospholipid modified glassy carbon electrode – determination of paraquat, J. Electroanal. Chem. 821 (2018) 33–39.
[21] H. Svecova, J. Souckova, M. Pyszkova, J. Svitkova, J. Labuda, J. Skopalova, P. Bartak, Phospholipids improve selectivity and sensitivity of carbon electrodes: determination of pesticide paraquat, J. Lipid Sci. Technol. 116 (2014) 1247–1255.
[22] C. Kalinke, A.S. Mangrich, L.H. Marcolino-Junior, M.F. Bergamini, Carbon paste electrode modified with biochar for sensitive electrochemical detection of paraquat, Electroanalysis 28 (2016) 764–769.
[23] M.A. El Mhammedi, M. Achak, M. Bakasse, R. Bachirat, A. Chitaint, Accumulation and trace measurement of paraquat at kaolin-modified carbon paste electrode, Mater. Sci. Eng. C 30 (2010) 833–838.
[24] J.O. Otalvaro, M. Brigante, Interaction of pesticides with natural and synthetic solids. Evaluation in dynamic and equilibrium conditions, Environ. Sci. Pollut. Res. 25 (2018) 6707–6719.
[25] J.O. Vinhal, C.F. Lima, R.J. Casella, Polyurethane foam loaded with sodium docecylsulfate for the extraction of 'quat' pesticides from aqueous medium, optimization of loading condition, Ecotoxicol. Environ. Saf. 131 (2016) 72–78.
[26] M. Brigante, M. Avena, Synthesis characterization and application of a hexagonal mesoporous silica for pesticide removal from aqueous solution, Microporous Mesoporous Mater. 191 (2014) 1–9.
[27] C.C. Harley, A.D. Rooney, C.B. Breslin, The selective detection of dopamine at a polypyrrole film doped with sulfonated β–cyclodextrins, Sensors Actuators B Chem. 150 (2010) 498–504.
[28] G. Bidan, C. Lopez, F. Mendes-Viegas, E. Vieil, A. Gadelle, Incorporation of sulfonated cyclodextrins into polypyrrole: an approach for the electro–controlled delivering of neutral drugs, Biosens. Bioelectron. 10 (1995) 219–229.
[29] S. Suematsu, Y. Oura, H. Tsujimoto, H. Kanno, K. Naoi, Conducting polymer films of cross-linked structure and their QCM analysis, Electrochim. Acta 45 (2000) 3813–3821.
[30] Y. Ling, J.T. Mague, A.E. Kaifer, Inclusion complexation of diquat and paraquat by the hosts cucurbit[7]uril and cucurbit[8]uril, Chem. Eur. J. 13 (2007) 7908–7914.
[31] T. Matsue, D.H. Evans, T. Osa, N. Kobayashi, Electron–transfer reactions associated with host–guest complexation. Oxidation of ferrocenecarboxylic acid in the presence of β–cyclodextrin, J. Am. Chem. Soc. 107 (1985) 3411–3417.
[32] E. Argyropoulou-Coutouli, A. Kelaidopoulou, C. Sideris, G. Kokkinidis, Electrochemical studies of ferrocene derivatives and their complexation by β–cyclodextrin, J. Electroanal. Chem. 477 (1999) 130–139.
[33] H. Dodziuk, Cylodextrins and Their Complexes, Wiley–VCH, 2006.